ELSEVIER

Chemical Geology 182 (2002) 637–654

CHEMICAL GEOLOGY
INCLUDING
ISOTOPE GEOSCIENCE

www.elsevier.com/locate/chemgeo

A geochemical traverse across the Eastern Carpathians (Romania): constraints on the origin and evolution of the mineral water and gas discharges

O. Vaselli [a,b,*], A. Minissale [b], F. Tassi [a], G. Magro [c], I. Seghedi [d], D. Ioane [d], A. Szakacs [d]

[a] *Department of Earth Sciences, University of Florence, Via G. La Pira, 4, I-50121 Florence, Italy*
[b] *CNR—Study Center for Mineralgenesis and Applied Geochemistry, Via G. La Pira, 4, I-50121 Florence, Italy*
[c] *CNR—Institute of Geochronology and Isotope Geochemistry, Via Alfieri 1, Località San Cataldo, 57017 Ghezzano, Pisa, Italy*
[d] *Geological Institute of Romania, Str. Caransebes, 1, RO-78344 Bucharest 32, Romania*

Received 21 June 2000; accepted 24 June 2001

Abstract

The inner sector of the Eastern Carpathians displays a large number of Na–HCO_3, CO_2-rich, meteoric-originated cold springs (soda springs) and bore wells, as well as dry mofettes. They border the southern part of the Pliocene–Quaternary Calimani–Gurghiu–Harghita (CGH) calc-alkaline volcanic chain. Both volcanic rocks and CO_2-rich emissions are situated between the eastern part of the Transylvanian Basin and the main east Carpathian Range, where active compression tectonics caused diapiric intrusions of Miocene halite deposits and associated saline, CO_2-rich waters along active faults. The regional patterns of the distribution of CO_2 in spring waters (as calculated pCO_2) and the distribution pattern of the $^3He/^4He$ ratio in the free gas phases (up to 4.5 R_m/R_a) show their maximum values in coincidence with both the maximum heat-flow measurements and the more recent volcanic edifices. Moving towards the eastern external foredeep areas, where oil fields and associated brines are present, natural gas emissions become CH_4-dominated. Such a change in the composition of gas emissions at surface is also recorded by the $^3He/^4He$ ratios that, in this area, assume 'typical' crustal values ($R_m/R_a = 0.02$).

In spite of the fact that thermal springs are rare in the Harghita volcanic area and that equilibrium temperature estimates based on geothermometric techniques on gas and liquid phases at surface do not suggest the presence of shallow active hydrothermal systems, a large circulation of fluids (gases) is likely triggered by the presence of mantle magmas stored inside the crust. If total ^3He comes from the mantle or from the degassing of magmas stored in the crust, CO_2 might be associated to both volcanic degassing and thermometamorphism of recently subducted limestones.

Keywords: Carpathian–Pannonian Region; Romania; Water–rock interaction; Water and gas geochemistry; He isotopes

1. Introduction

After the basic studies on the carbon cycle by Berner et al. (1983) and Berner and Lasaga (1989), a

* Corresponding author. Department of Earth Sciences, University of Florence, Via G. La Pira, 4, I-50121 Florence, Italy. Tel.: +39-55-2756289; fax: +39-55-284571.
E-mail address: orlando@steno.geo.unifi.it (O. Vaselli).

0009-2541/02/$ - see front matter
PII: S0009-2541(01)00348-5

large number of papers have been published concerning the flux of CO_2 from active volcanic (e.g. Gerlach, 1991; Williams et al., 1992; Marty and Tolstikhin, 1998) and hydrothermal–volcanic-related (e.g. Brantley and Koepenick, 1995; Kerrick et al., 1995; Seward and Kerrick, 1996; Rogie et al., 2000) areas. Many of these papers have focused their attention to the deficit existing between CO_2 consumed by rock chemical weathering and endogenous CO_2 outgassing to the atmosphere. To this budget calculations, only few studies have dealt with CO_2 dissolved in groundwater (Chiodini et al., 1999, 2000), which might represent a relevant contribution to the carbon cycle, even in areas not related to active volcanism. In fact, unlike free CO_2 that discharges close to its source (either volcanic or hydrothermal), dissolved CO_2 can laterally be transported by solutions underground in the presence of a well-developed convective circulation (Minissale et al., 2000b; Polyak et al., 2000).

The Eastern Carpathians have experienced subduction-related andesitic volcanism in the past 13–0.035 Ma (Pesckay et al., 1995; Mason et al., 1996; Moriya et al., 1996) and still exhibit present heat-flow anomalies, as reported in the volcanic area (Veliciu, 1987). Although no active volcanoes and fumaroles are present around the more recent volcanic edifices in the Harghita Mountains belonging to the Calimani–Gurghiu–Harghita (CGH) calc-alkaline volcanic chain, a large number of CO_2-rich cold springs (soda springs), as well as dry mofettes, discharge abundant CO_2 to the surface and the atmosphere. Some thermal waters were described in wells in the volcanic area by Radulescu et al. (1981) and Craciun and Bandrabur (1993). In addition, CO_2 emissions, in places in association with saline waters, spread also over the main Carpathians thrust belt zone along active faults.

Following guidelines settled in the Northern Apennines (central–northern Italy; Minissale et al., 2000b) and Northern Caucasus (Polyak et al., 2000), a fluid-geochemical investigation has been carried out on spring and well waters, as well as dry gases across another active plate boundary area such as the Eastern Carpathians. The main purpose is to establish the origin of such cold CO_2 emissions, meaning of gas and water samples from a geothermal point of view, and relations with the Harghita Mountains volcanism and the present geological structural setting of the area.

2. Geological background

The present shape of the Carpathian Chain resulted from the convergence between African intra-Carpathian blocks (Alcapa and Tisia–Dacia microplates) and the Eurasian plate, driven by Miocene–Pliocene subduction retreat (e.g. Royden, 1993; Csontos, 1995; Mason et al., 1998; Seghedi et al., 1998). This collision produced folding and thrusting of Cretaceous–Neogene flysch successions, presently northward trending (Fig. 1), with an eastern outward vergence (Sandulescu, 1984; Roman, 1970). This northward trend in the Eastern Carpathians changes strike by 80° towards west, in a bend zone located very close to the seismic Vrancea region, where a slab delamination model has been adopted to explain its deep-seated seismicity (Bleahu, 1985; Garbacea, 1997).

The area under study is located between the internal Transylvanian Basin to the west and the external Focsani foredeep basin to the east and is crossed by the southern segment of the CGH andesitic volcanic chain. This subduction-related calc-alkaline activity migrated in time from north to south (Radulescu et al., 1972; Peltz et al., 1987; Pecskay et al., 1995) to accommodate the diachronous break-off processes (Mason et al., 1998; Seghedi et al., 1998). The youngest volcanic activity of the Ciomadul volcano, in the southernmost part of the CGH, is still a matter of debate since it dates back to 10.7 ka (Juvigne et al., 1994) or 35–42 ka (Moriya et al., 1996).

Among other tectonic features, piggyback basins formed during the main Miocene overthrusting of the flysch units and they are presently spread throughout the whole area (Zweigel, 1997). As a consequence of the ongoing deformative process, salt diapirism occurred in both the internal and external sectors of the chain (Mrazec, 1907). Such diapirs are mined for halite (e.g. the Praid–Corund area in the Transylvanian Basin; Fig. 1) or are associated to saline waters and used in Spa (e.g. Slanic area in the main thrust belt zone; Fig. 1). In the Vrancea region, saline waters are associated to CH_4-rich mud volcanoes,

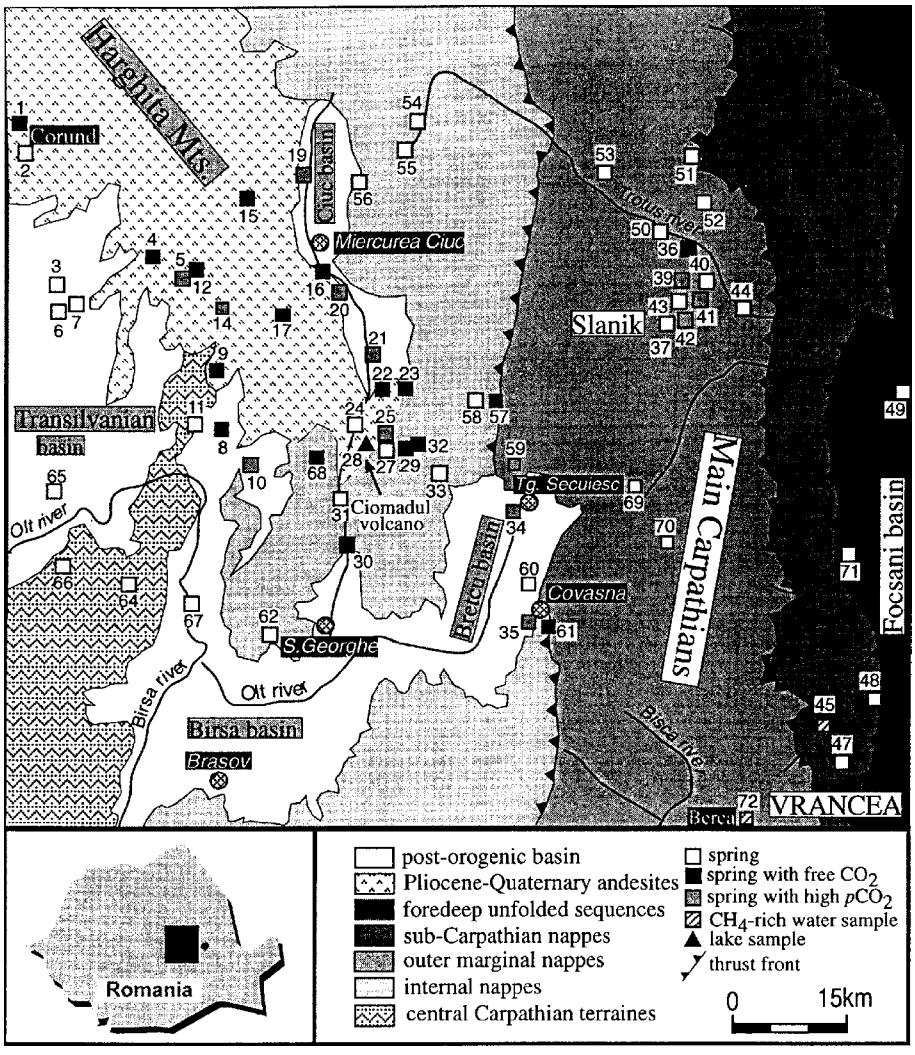

Fig. 1. Schematic geological map of the southeastern Carpathians with location of sampling points.

and more generally to the presence of oil fields (Baltes, 1983).

From a hydrogeological point of view, the main Carpathian belt and the Harghita Mountains (with maximum elevation range of 1500–1900 m) are heavy-rain areas, with a snow cap that lasts for 3–4 months in winter. According to the lithological features, infiltration capacity and permeability, as inferred from flow rates of springs, is more reduced in the flysch areas and quite variable in the different massive and volcanoclastic deposits of the Harghita area (Craciun and Bandrabur, 1993). As a consequence, a large number of both CO_2-rich and CO_2-free springs discharge at the contact between the volcanics and the flysch series and where the volcanic cover is reduced (Fig. 1).

According to Veliciu (1987, 1988), this sector of the CGH volcanic chain hosts the strongest heat-flow anomaly in Romania (85–120 mW m^{-2}). The deepest measured temperature is up to 78 °C at 1140 m in a drillhole at Baile Tusnad, near the Ciomadul volcano (Radulescu et al., 1981). On the basis of heat-flow data and the age of volcanic activity of the CGH, the modeling of geothermal anomalies in the

east Carpathians has suggested that: (i) 1/5–1/4 of the surface heat flow originates from a mantle source related to the subduction process, (ii) 2/3 is related to radiogenic heat generated in the crust, and (iii) the remaining contribution is due to still cooling magma chambers in the crust (Radulescu et al., 1983).

3. Sampling and analytical methods

Temperature, pH, electrical conductivity, HCO_3, NH_4, and SiO_2 in the water samples were measured in the field, whereas the remaining components were determined in the laboratory according to the analytical methods reported in Duchi et al. (1986). $^{18}O/^{16}O$ and $^{2}H/^{1}H$ isotopic ratios (expressed as $\delta^{18}O$ and δD ‰ SMOW) were determined with a Finningan 250 delta mass spectrometer after equilibrating the waters with CO_2 and after the reaction of 10 ml of water with 0.3 g of pure Zn at 500 °C, respectively.

Gas emissions were convoyed with a funnel positioned upside down in the water discharges, or directly above the vent in the case of dry mofettes, into two types of pre-evacuated vacuum vials: a thorion-tapped tube (100 cm^3 in volume) for CO_2, N_2, and CH_4 determinations and a thorion-tapped tube (50 cm^3 in volume), prefilled with 25 ml of 4 N NaOH (Giggenbach, 1975), for permanent gases analyses, including hydrocarbons.

Gas species were analysed by gas chromatography using thermal conductivity (CO_2, N_2, O_2, H_2S, He, Ar, and H_2) or flame ionization (CH_4 and CO) detectors. The ^{4}He, ^{20}Ne, and ^{22}Ne were analysed in a static way by using a Spectrolab 200 VG-Micromass quadrupole mass spectrometer (Magro and Pennisi, 1991). $^{3}He/^{4}He$ ratios were determined with a Map 215-50 magnetic mass spectrometer. No blank corrections were carried out because the He content of the samples was several orders of magnitude higher than that of the extraction line and the instrumental static background. Generally speaking, the analytical errors were $< 10\%$ for the abundances and $< 5\%$ for the isotopic ratios. $^{13}C/^{13}C$ isotopic ratios in CO_2 (expressed as $\delta^{13}C$ ‰ PDB) were determined with a Finningan 250 delta mass spectrometer after the standard procedures of extraction and purification of the gas mixture.

Sampling sites, according to the type of associated gas phase, are reported in Fig. 1, whereas chemical and isotopic data of water and gas samples are shown in Tables 1 and 2, respectively.

4. Chemistry of waters

By plotting the main components in solution in the Langelier–Ludwig diagram (Fig. 2), the great majority of samples is confined in a triangle where the composition of typical Ca–HCO_3 running and ground waters, the Na–Cl composition of waters deriving from halite dissolution, and the composition of Na–HCO_3 waters are at the vertexes. Samples in the groundwater corner are relatively low-salinity waters (generally < 1000 mg/kg), whereas some of those lying in the Na–Cl corner are extremely saline ($> 50{,}000$ mg/kg; nos. 1, 47, and 72 in Table 1). From the line joining these two groups, a shift towards the Na–HCO_3 corner is clearly seen and likely related to the presence of free-rising CO_2 favouring the increase of the Na–HCO_3 component in solution (e.g. Drever, 1982).

Dissolved carbon dioxide, calculated as pCO_2 using the speciation program WATEQ4F (Ball and Nordstrom, 1991), plotted against salinity (TDS = total dissolved salts), clearly divides the water samples in three groups (Fig. 3):

1. samples with $pCO_2 < -1$ and $150 < TDS < 2000$ mg/kg;
2. samples with relatively high TDS ($> 10{,}000$ mg/kg) and $-1.5 < pCO_2 > -1.0$; and
3. samples with pCO_2 varying from -0.5 to more than $+0.5$ and extremely variable TDS from 100 to over 200,000 mg/kg.

Samples belonging to the first group are mainly characterised by surficial waters (e.g. nos. 64, 69, 49, 27, etc.), although within this group, gas pool-bearing waters are present (e.g. nos. 12, 45, 51, and 71). Group 2 includes high-salinity waters mainly related to an associated gas phase. Samples with high pCO_2 (group 3) are scattered in all the sectors of the Langelier–Ludwig diagram, no matter whether salinity derives from water–silicate/carbonate interaction processes in different aquifers or simple halite dissolution in diapire-related waters (nos. 1, 35, 36, 39, 41, 42, 42, and 61).

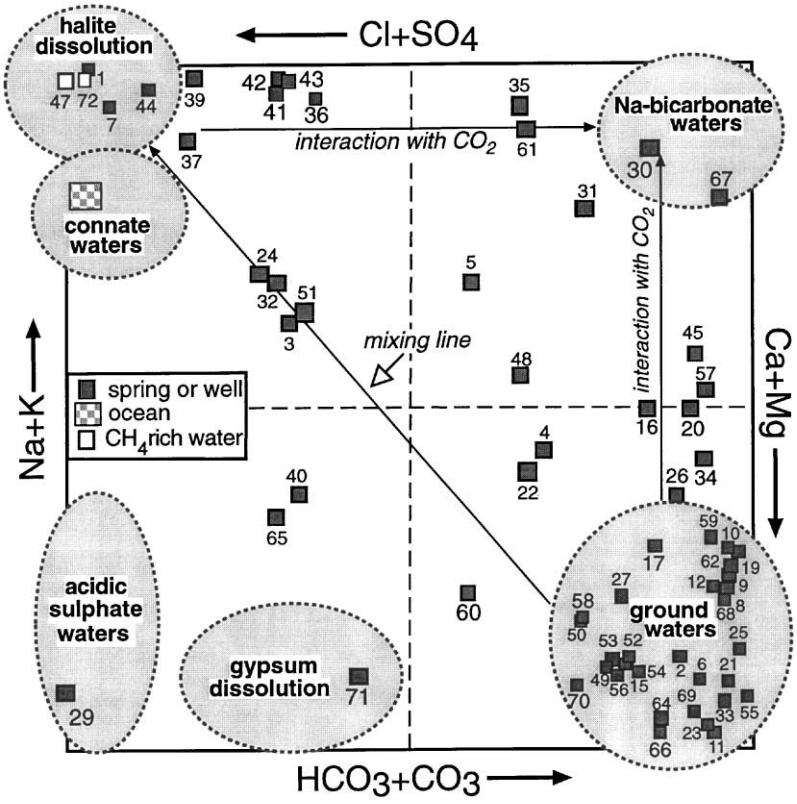

Fig. 2. Langelier–Ludwig diagram for the water samples investigated.

On the other hand, the saline waters discharge ubiquitously: in the eastern part of the Transylvanian Basin (no. 1), along the main trust belt area (nos. 39, 42–44, and 61), as well as in the foredeep area (nos. 47 and 72).

From a genetic point of view, the cross comparison of $\delta^{18}O$–δD (Fig. 4a), Cl–δD (Fig. 4b), Cl–$\delta^{18}O$ (Fig. 4c), and $\delta^{18}O$-spring discharge elevation (Fig. 4d) suggests that, setting aside the very saline samples where $\delta^{18}O$ and δD are available (nos. 1, 30, 31, 35, 36, 39, 47, 61, and 72), most water samples in the study area clearly have a meteoric origin. Generally speaking, $\delta^{18}O$ varies, on the average, from $-8.0‰$ to $-12.0‰$ (SMOW) with many samples in the range $-10‰$ to $-12‰$, corresponding to rainfalls at 1000–2200 m in elevation (Fig. 4c and d) (Craig, 1961; Gatt and Carmi, 1970).

Very saline waters (nos. 1 and 72, Table 1) show in the $\delta^{18}O$–δD diagram (Fig. 4a) a wide oxygen shift. By looking at the Cl–$\delta^{18}O$ diagram (Fig. 4c), it would come out that these saline samples, being much more saline that seawater, could have been formed in association with evaporites precipitation during the Messinian salinity crisis and increased the isotopic $^{18}O/^{16}O$ ratio after evaporation. On the other side, because its D/H ratio is lower than present seawater (Fig. 4b), evaporation processes must be excluded. A mixing between connate and meteoric waters and contemporary dissolution of Miocene halite seems to be the more likely process, where the marked ^{18}O shift is caused by the very high salinity of solutions that brings light molecules of water to be more tight bound to the ions in solution (Gonfiantini, 1986). Mixing of low-salinity waters flowing from the Carpathians with saline waters from the low-elevation Transylvanian (no. 1) and Focsani (no. 72) basins seems to be justified by the mixing line shown in Fig. 4d. Sample no. 28,

Table 1
Chemical (in meq/l) and isotopic (in ‰ SMOW) composition of water samples from the Eastern Carpathians

No.	Site	Type	Elevation	T (°C)	pH	pCO_2	TDS	HCO_3	Cl	SO_4	Ca	Mg	Na	K	NH_4	Li	NO_3	F	Br	SiO_2	B	$\delta^{18}O$	δD
1	Corund Nord	sg	200	16.4	6.58	0.28	177 228	106.70	2875	24.17	1.23	17.94	2923	26.23	6.280	11.110	< 0.0002	0.0895	0.9387	0.271	12.000	7.23	− 25.6
2	Corund Village	s	700	13.1	5.88	− 0.54	358	4.31	0.4	0.13	2.51	1.23	0.5	0.11	0.056	0.0009	0.0002	0.0026	< 0.0001	0.850	0.009	− 9.83	nd
3	Szekely	gp	560	13.0	6.17	− 0.28	3538	17.60	35.1	1.08	18.40	2.20	33.5	0.30	0.096	0.0381	< 0.0002	0.0105	0.0213	0.132	0.089	− 9.90	nd
4	Homorod Maria	gp	750	11.2	6.03	− 0.03	2272	22.27	9.6	0.01	7.83	9.71	13.0	0.55	0.034	0.0607	< 0.0002	0.0026	0.0013	1.017	0.409	− 11.30	nd
5	Vlahita Logobo	gp	850	18.0	5.96	− 0.05	1903	16.13	11.0	0.01	4.54	3.80	17.0	0.75	0.050	0.1184	< 0.0002	0.0211	0.0025	1.075	1.155	− 10.17	nd
6	Fata Padurii	s	nd	11.0	7.86	− 2.36	578	6.68	0.1	0.47	6.23	0.64	0.5	0.22	0.003	0.0023	0.0339	0.0037	< 0.0001	0.108	0.009	− 10.22	nd
7	Soskut	gp	650	13.5	7.25	− 1.62	9004	10.00	141.5	0.50	5.84	3.36	138.7	0.88	0.383	0.0879	< 0.0002	0.0421	0.0363	0.104	0.720	− 8.73	nd
8	Doboseni	gp	550	12.1	5.96	− 0.07	1318	16.40	0.6	0.01	8.28	4.18	3.4	0.33	0.036	0.0547	0.0040	0.0184	0.0009	1.008	0.415	− 11.45	nd
9	Piriul Capelei	w	nd	17.0	5.78	0.09	1171	14.67	0.5	0.00	6.93	3.65	3.3	0.24	0.039	0.0471	0.0008	< 0.003	< 0.0001	1.067	0.266	− 11.46	nd
10	Biborteni	gp	nd	14.5	5.95	0.12	2091	25.30	1.5	0.13	12.27	6.19	7.3	0.80	0.228	0.1101	0.0194	0.0263	0.0025	0.992	0.905	− 11.45	nd
11	Kis	s	nd	9.5	7.29	− 1.81	523	6.27	0.1	0.28	5.74	0.59	0.1	0.02	0.004	0.0010	0.0306	0.0032	0.0002	0.129	0.002	− 10.92	nd
12	Perla Vlahitei	ts	900	26.0	6.86	− 1.37	418	5.20	0.1	0.23	2.07	1.86	1.0	0.22	0.004	0.0054	0.0003	0.0026	< 0.0001	1.158	0.008	− 10.87	nd
14	Baile Chirui	gp	nd	12.7	5.79	0.06	1265	14.67	1.7	0.15	5.89	4.26	5.7	0.33	0.022	0.0410	< 0.0002	0.0053	0.0006	0.975	0.253	− 11.82	nd
15	Harghita Bai	s	950	7.5	5.27	− 0.37	129	1.60	0.1	0.29	0.34	0.47	0.1	0.02	0.004	0.0011	< 0.0002	0.0632	< 0.0001	0.158	0.003	− 11.01	− 79.5
16	Jigodin Bai	gp	750	18.8	5.72	0.29	1804	20.40	3.5	0.05	6.28	4.76	10.9	0.50	0.067	0.1226	< 0.0002	0.0053	0.0041	1.158	1.014	− 11.12	nd
17	Sintimbru Bai	s	975	7.5	5.26	− 0.33	142	1.69	0.1	0.23	0.64	0.40	0.4	0.05	0.008	0.0007	0.0006	0.0195	< 0.0001	0.483	0.010	− 11.16	nd
19	Racu	gp	nd	11.3	5.80	− 0.01	1005	12.80	0.3	0.09	4.97	3.69	2.8	0.29	0.007	0.0186	< 0.0002	< 0.003	< 0.0001	1.058	0.106	− 11.26	nd
20	Jigodin Bai 2	w	nd	19.0	5.96	− 0.04	1372	16.13	1.5	0.04	4.99	3.79	8.0	0.38	0.050	0.1013	< 0.0002	0.0053	0.0025	1.208	0.736	− 11.25	nd
21	Cetatuia	w	nd	11.0	5.90	0.01	1700	21.10	0.8	0.01	15.09	3.46	1.8	0.18	0.103	0.0303	< 0.0002	0.0026	< 0.0001	0.825	0.078	− 10.64	nd
22	Tusnad Nadas	gp	nd	17.5	6.83	− 0.10	1822	17.47	8.4	0.02	7.93	6.68	9.4	0.40	0.046	0.1116	< 0.0002	0.0158	0.0088	1.050	0.578	− 10.73	− 77.9
23	Lazaresti Nyir	s	750	11.0	5.96	− 0.31	793	9.46	0.1	0.56	8.48	0.91	0.2	0.06	0.038	0.0033	0.0048	< 0.003	< 0.0001	0.333	0.009	− 10.71	nd
24	Tusnad Bai	gp	nd	16.2	5.72	− 0.18	1470	7.06	16.9	0.01	4.84	2.12	13.7	2.02	0.278	0.2507	< 0.0002	0.0105	0.0219	1.075	1.682	− 10.70	nd
25	Jimbor	s	nd	9.2	5.50	0.08	586	7.80	0.1	0.03	3.77	1.07	0.7	0.12	0.038	0.0094	< 0.0002	0.0047	0.0001	0.550	0.020	nd	nd
27	Cantonului	s	nd	11.2	7.52	− 2.66	130	1.40	0.0	0.29	1.03	0.23	0.3	0.08	0.016	0.0017	0.0002	0.0053	0.0001	0.742	0.007	nd	nd
29	Puturosul Sud	w	850	11.2	2.22	0.00	1175	0.00	0.1	20.73	7.03	1.95	0.5	0.28	0.067	0.0066	< 0.0002	0.0089	< 0.0001	0.521	0.051	− 10.26	nd
30	Bodoc Pella	gp	700	10.8	6.35	0.10	5904	64.60	11.1	0.05	2.02	7.28	62.5	1.48	0.300	0.1430	0.0242	0.0053	0.0163	0.275	4.727	− 5.72	− 70.0
31	Malmas Bay	gp	600	11.0	6.47	− 0.09	5630	55.70	17.6	0.20	12.22	3.29	57.1	1.11	0.306	0.5014	0.0403	0.0105	0.0213	0.508	7.318	− 5.04	nd
32	Balvanyus	gp	850	9.3	5.82	− 0.17	2153	9.87	12.4	9.79	7.38	2.58	20.0	0.92	0.046	0.2689	< 0.0002	0.0053	0.0238	0.225	1.727	− 11.49	− 75.4
33	Zsofia	s	nd	9.0	5.84	− 0.26	623	7.94	0.1	0.19	5.24	0.88	0.4	0.06	0.017	0.0060	< 0.0002	0.0063	< 0.0001	0.267	0.014	− 11.40	nd
34	Fortyogo	s	540	10.2	5.55	0.07	719	8.70	0.6	0.00	3.30	1.60	3.5	0.09	0.015	0.0246	0.0002	< 0.003	0.0014	0.517	0.110	− 10.90	nd
35	Covasna	w	600	10.8	6.34	0.16	8364	74.90	37.5	0.25	1.94	5.31	102.0	3.54	0.794	0.8429	< 0.0002	0.0158	0.0626	0.292	10.227	− 3.35	− 49.1

36	Slanic − 15	gp	660	10.0	6.40	− 0.02	10 777	59.00	102.0	0.05	5.59	2.72	148.1	3.44	0.933	0.3971	< 0.0002	0.0526	0.0313	0.104	4.545	− 6.69	− 67.6
37	Slanic − 5	s	650	9.0	4.73	− 0.21	237	0.67	1.5	1.54	0.21	0.15	2.7	0.16	0.024	0.0209	< 0.0002	0.0084	< 0.0001	0.233	0.095	− 9.69	nd
39	Slanic W2	w	550	8.7	6.20	0.28	25 905	77.00	339.0	0.25	2.64	4.53	393.4	6.51	2.096	0.7414	< 0.0002	0.1684	0.1564	0.050	8.909	− 2.61	− 56.9
40	Slanic fountain	w	nd	10.0	5.06	− 0.75	80	0.40	0.0	0.72	0.48	0.22	0.3	0.12	0.005	0.0041	0.1516	0.0021	0.0001	0.342	0.017	nd	nd
41	Slanic 1	gp	650	9.5	6.15	0.18	11 365	52.80	118.1	1.04	3.84	1.60	165.4	0.28	0.756	nd	< 0.0002	< 0.003	0.0250	nd	nd	− 11.00	nd
42	Slanic 6	gp	nd	12.0	6.63	− 0.10	17 840	84.39	185.8	1.01	7.21	4.88	253.9	3.79	1.235	nd	< 0.0002	< 0.003	0.0313	nd	nd	nd	nd
43	Slanic 14	gp	nd	10.3	6.53	− 0.05	15 679	74.00	163.0	0.33	1.50	3.95	229.6	4.97	1.694	0.5821	< 0.0002	0.0263	0.0782	0.133	7.273	− 4.37	nd
44	Targu Ocna	gp	450	11.0	7.22	− 1.30	10 047	20.27	144.1	0.67	3.39	2.73	154.8	0.23	0.444	0.0161	< 0.0002	0.0632	0.0438	0.150	0.214	− 11.10	− 67.4
45	Andreasu	mc	700	12.0	7.10	− 1.32	1073	12.53	0.8	0.33	3.59	2.05	7.3	0.25	0.046	0.0121	0.1935	0.0095	0.0025	0.275	0.020	− 7.22	nd
47	Piriul Sarat	gp	700	7.5	7.50	− 1.38	307 215	8.28	5200	62.50	94.20	28.07	5081	4.40	2.569	0.2070	0.3050	0.211	1.2500	0.067	3.800	− 5.79	nd
48	Reghiu	gp	800	7.1	8.01	− 2.41	1034	8.93	0.1	4.38	3.95	2.27	7.3	0.09	0.017	0.0030	0.0570	0.008	< 0.0001	0.050	0.034	− 10.39	nd
49	Urechesti	w	nd	7.7	8.20	− 2.71	660	6.91	0.6	1.20	5.80	1.81	1.0	0.10	0.01	0.0010	0.0020	0.005	0.0019	0.083	<	− 10.79	nd
50	Bogata	w	nd	5.7	7.87	− 2.47	553	5.49	0.7	1.15	5.20	0.65	1.2	0.10	0.014	0.0010	< 0.0002	0.003	0.0001	0.100	0.032	− 10.96	− 73.6
51	Moinesti	gp	750	10.8	6.97	− 1.28	2042	10.88	18.4	1.88	8.55	2.47	18.9	0.58	0.018	0.0040	0.0850	0.024	0.0238	0.125	0.014	− 9.65	nd
52	Comanesti	s	nd	8.7	7.57	− 2.07	625	6.77	1.3	0.19	5.50	1.88	1.1	0.04	0.011	0.0010	0.1610	0.005	0.0006	0.167	0.004	− 11.99	nd
53	Beleghet	w	nd	7.3	7.61	− 2.25	478	4.95	0.4	0.87	4.70	0.94	0.7	0.13	0.014	0.0010	0.3630	0.003	0.0003	0.050	0.012	− 10.50	nd
54	Lunca de Mijlok	w	nd	7.3	7.80	− 2.49	415	4.34	0.3	0.57	4.85	0.48	0.4	0.21	0.017	< 0.001	0.8060	0.008	0.0001	0.067	0.006	nd	nd
55	Vraja Muntilor	gp	nd	12.8	6.30	− 0.33	1593	20.08	0.1	0.01	13.55	5.00	1.4	0.11	0.013	0.0090	0.0050	0.016	< 0.0001	0.142	0.008	− 11.50	nd
56	Frumoasa	w	nd	5.0	7.88	− 2.38	714	7.18	1.0	0.78	8.60	0.68	1.0	0.02	0.016	0.0010	1.6940	0.003	0.0001	0.100	0.004	− 10.60	nd
57	Perla Casinului	gp	800	7.7	6.39	− 0.17	4826	56.75	4.0	0.02	24.25	3.91	29.9	0.64	0.306	0.0680	0.0160	0.003	0.0160	0.933	1.832	− 8.53	nd
58	Iacobeni	w	nd	5.3	7.69	− 2.18	729	7.24	0.8	1.56	6.55	1.05	1.8	0.03	0.02	0.0010	0.0890	0.008	0.0001	0.100	0.018	− 9.94	nd
59	Poian	w	750	10.1	5.98	0.33	3925	48.39	0.9	0.10	25.90	9.14	13.4	0.58	0.257	0.0590	0.0320	0.005	< 0.0001	0.700	0.636	− 10.31	nd
60	Zabala	w	610	7.8	7.56	− 2.13	749	5.90	2.2	1.98	6.65	2.25	2.5	0.11	0.018	< 0.001	1.3400	0.008	0.0013	0.150	0.062	− 10.44	nd
61	Covasna	gp	nd	12.6	6.43	0.16	9956	90.95	44.0	0.20	4.50	8.31	114.9	3.31	0.004	0.4990	0.8580	0.021	0.0830	0.125	10.636	− 3.20	nd
62	Vilcele	gp	700	11.0	6.67	− 0.30	4494	55.62	1.9	0.01	16.55	25.60	16.9	0.28	0.087	0.1410	0.0400	0.013	0.0090	0.417	0.197	− 10.97	− 83.8
64	Caprioara	s	nd	6.8	8.24	− 2.99	341	3.80	0.0	0.54	3.65	0.46	0.1	0.04	0.016	< 0.001	0.0210	0.003	0.0001	0.133	0.024	− 9.96	nd
65	Homorod	w	600	8.6	7.21	− 1.55	2472	10.75	14.4	9.90	23.55	3.66	13.7	0.20	0.319	0.0060	6.8550	0.145	0.0038	0.108	0.046	− 9.02	nd
66	Fintina	s	nd	8.7	7.70	− 2.32	464	5.08	0.1	0.73	5.60	0.24	0.1	0.02	0.016	< 0.001	0.0480	0.003	0.0001	0.100	0.007	− 10.56	nd
67	Maierus	w	650	24.6	7.88	− 2.34	502	5.89	0.3	0.00	0.92	0.30	4.8	0.09	0.944	0.0070	0.0280	0.005	0.0006	0.267	0.040	− 12.72	nd
68	Ozunca Bai	s	800	9.7	5.84	− 0.04	509	6.32	0.2	0.03	2.83	2.21	1.3	0.07	0.009	0.0060	0.0500	0.005	0.0001	0.900	0.047	− 10.74	− 79.1
69	Vrancea Pass	s	950	6.0	8.35	− 3.20	262	3.05	0.0	0.26	2.95	0.15	0.1	0.10	0.017	< 0.001	0.0730	0.003	< 0.0001	0.050	0.013	− 12.09	− 89.3
70	Gresu	w	nd	8.6	7.69	− 2.34	513	4.76	0.9	0.76	6.88	0.35	0.6	0.10	0.014	< 0.001	1.7900	0.003	0.0006	0.067	0.011	− 10.80	nd
71	Vizantea	gp	500	10.3	7.06	− 1.50	1342	7.92	0.2	10.63	12.10	4.83	1.8	0.14	0.031	0.0100	0.0430	0.008	0.0006	0.183	0.054	− 10.09	nd
72	Berca	mc	200	12.0	7.48	− 1.43	58 051	28.46	960.0	1.88	5.50	16.54	949.1	3.77	1.333	0.7390	0.1210	< 0.003	0.9000	0.067	25.182	5.81	− 25.8

s = Spring; sg = spring with associated gas; w = well; mv = mud volcano (CH_4 rich); gp = gas pool (CO_2 rich).

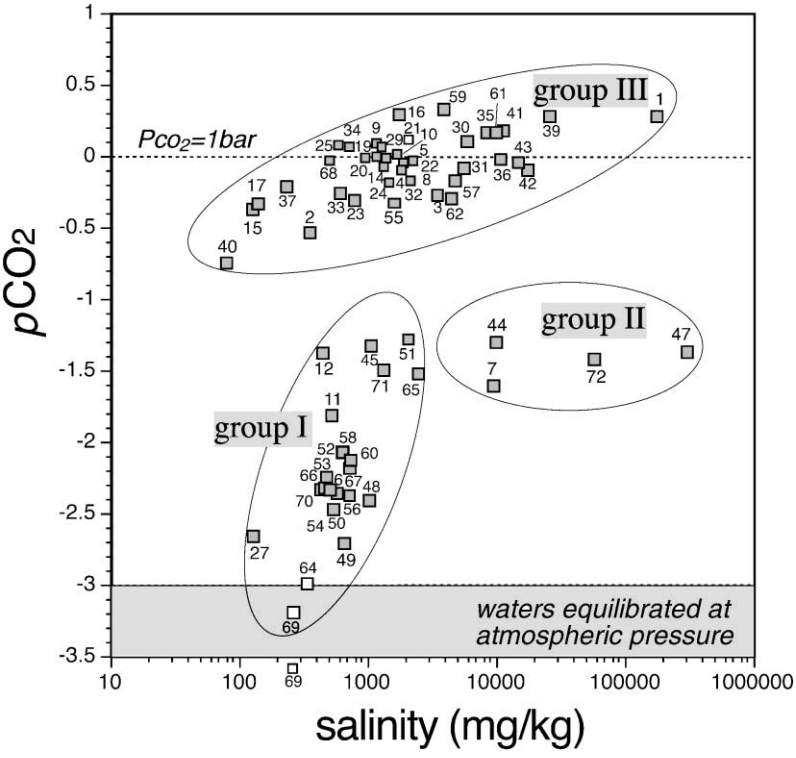

Fig. 3. pCO_2 vs. salinity diagram for the spring samples investigated. Three groups according to either salinity or pCO_2 have been recognised.

collected from the Sfinta Ana crater lake at the top of the Ciomadul volcano, seems to have undergone free surface evaporation (Fig. 4b and c).

5. Chemistry of gases

Apart from the CH_4-rich samples taken at Andreasu (no. 45) and Berca (no. 72) in the foredeep Focsani basin (Fig. 1), the latter being affected by the presence of mud volcanoes clearly connected to the presence of oil fields (Baltes, 1983), the remaining samples are CO_2 rich (up to 99.8% by volume in no. 57). The CO_2 vents are in the internal eastern sector of the Carpathians and prevalently related to the presence of the andesite volcanoes. Some gas samples have relatively high O_2 contents (nos. 8, 12, and 61 in Table 2), which can be due to either the presence of air in their very shallow pathways or cracks in the plumbing system at the emergence sites.

All gas samples have been plotted in the $N_2/100-He \times 10-Ar$ diagram (Fig. 5; after Giggenbach et al., 1983) together with the composition of potential sources of gases deriving from air ($N_2/Ar = 83$), air-saturated water (ASW, with $N_2/Ar = 38$ at 25 °C), andesite magma ($N_2/Ar = 800$; Giggenbach et al., 1983), and ^{4}He-enriched crustal gas. The gray triangle in the figure outlines the area where natural gases of any initial composition (N_2-CH_4 or CO_2 rich) maintain the N_2/Ar ratio between that in the air and ASW, and become enriched in radiogenic ^{4}He after progressive residence time in the crust (e.g. Xu et al., 1997; Minissale et al., 2000a) or mixing of young with old ground waters (Mazor, 1991). Several samples (nos. 15, 22, 17, 29a, 32, 30, 57, and 68) including the two CH_4-rich samples (nos. 45a and 72) have N_2/Ar values in the air/ASW ratios. On the contrary, other samples (nos. 1, 8, 9, 12, 16, 23, 28, 29b, 36, and 45) show N_2 enrichment where N_2 is not related to the atmosphere. Because the area

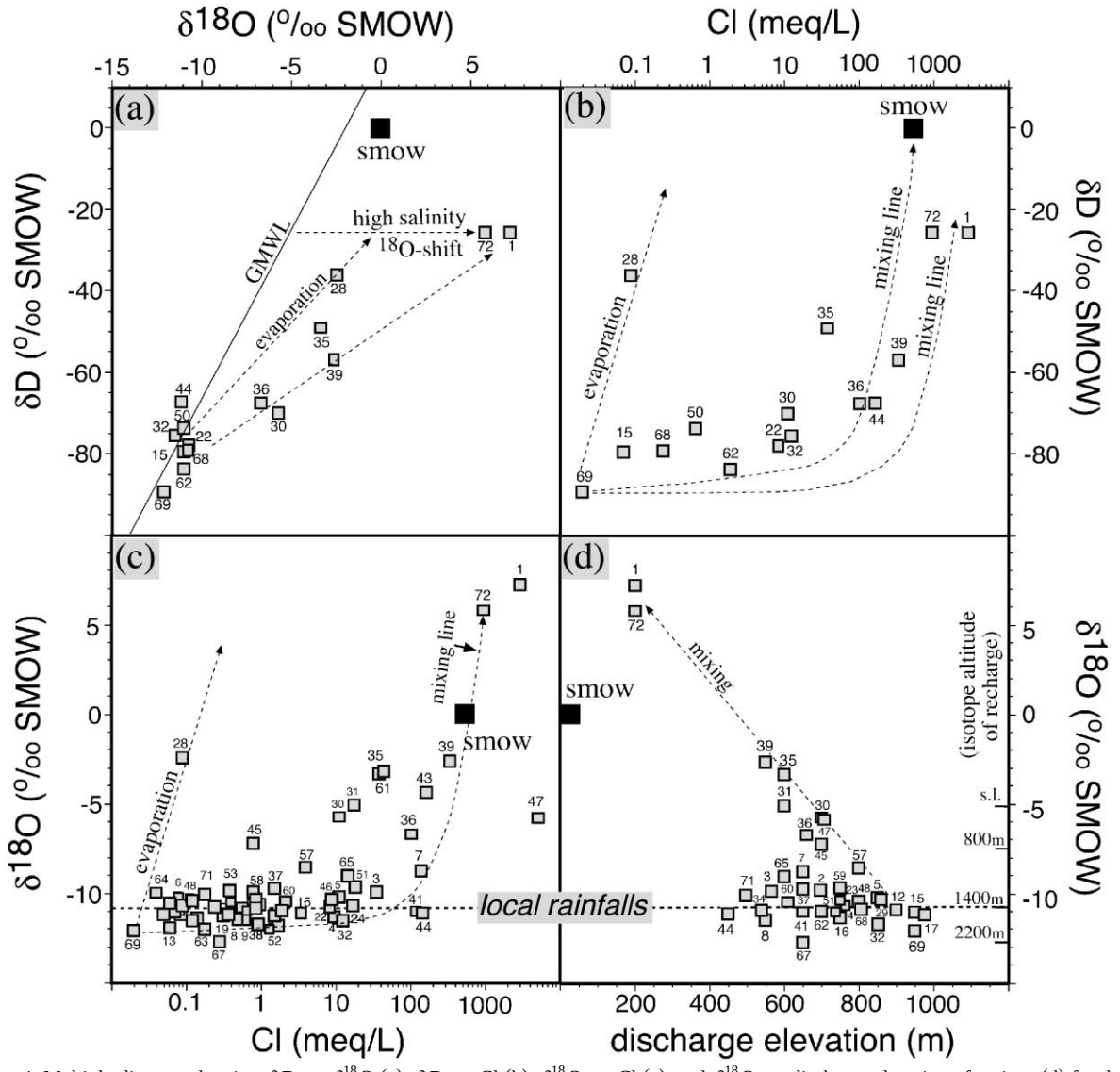

Fig. 4. Multiple diagram showing δD vs. δ^{18}O (a), δD vs. Cl (b), δ^{18}O vs. Cl (c), and δ^{18}O vs. discharge elevation of springs (d) for the sample investigated (see text).

hosts andesitic volcanics, it could be organic N_2 recycled from subducted sediments as suggested by Giggenbach (1983), still degassing from buried magma chambers.

The measured isotopic δ^{13}C in CO_2 values fall in the range -2.0‰ to -4.7‰ (PDB) and two samples (nos. 1 and 12) approach -10.0‰ (Table 2). The latter values can be related to the presence of CO_2 deriving from the alteration of isotopically light recent organic matter embedded in the Transylvanian Basin. The remaining 12 samples suggest a relatively uniform production of CO_2, possibly related to thermometamorphism of carbonate rocks, from a single, though likely mixed, deep source that, after spreading at shallow depth in the aquifers, favours the transfer of the gas phases to the atmosphere.

Table 2
Gas composition (percentage by volume) of samples from the southeastern Carpathians

No.	Località	CO_2	N_2	CH_4	Ar	O_2	He	H_2	H_2S	CO	$\delta^{13}C$ in CO_2	R_m / R_a	He/Ne	$^3He/^4He^a$
1	Corund	99.68	0.298	0.0019	0.0026	0.0052	0.000010	0.000154	0.017	< 0.000001	−9.18	0.87	1.71	0.84
4	Homorod Maria	98.24	1.159	0.3632	0.0380	0.2131	0.000266	0.000048	< 0.005	< 0.000001	−2.03	0.62	8.39	0.61
8	Doboseni	72.61	21.593	0.5424	0.1248	5.1318	0.002135	0.000001	< 0.005	< 0.000001	−3.25	4.27	8.87	4.38
9	Piriul Capelei	97.68	1.956	0.3372	0.0205	0.0032	0.000479	0.000014	< 0.005	< 0.000001	−3.49	1.74	25.60	1.75
12	Perla Vlahitei	15.30	75.325	0.0013	0.4810	9.0112	0.002855	0.000694	< 0.005	< 0.000001	−10.38	nd	nd	
15	Harghita Bai	98.79	0.975	0.1073	0.0191	0.1293	0.000083	0.000006	< 0.005	< 0.000001	−4.21	3.04	1.41	3.55
16	Jigodin Bai	98.84	0.989	0.0984	0.0040	0.0715	0.000081	0.000001	< 0.005	< 0.000001	−3.07	0.45	5.20	0.42
17	Sintimbru Bai	97.41	2.038	0.1073	0.0263	0.4330	0.000102	0.000049	< 0.005	< 0.000001	−2.14	1.26	1.08	1.35
22	Tusnad Nadas	99.56	0.327	0.0038	0.0067	0.1100	0.000006	0.000034	< 0.005	< 0.000001	−4.42	1.66	1.28	1.84
23	Lazaresti Nyir	89.11	7.411	3.3680	0.0345	0.1039	0.000780	0.000040	0.005	0.000022	nd	2.95	7.70	3.02
28	Sfinta Ana	97.69	1.612	0.6503	0.0026	0.0424	0.000694	0.000005	< 0.005	0.000007	nd	3.16	25.00	3.18
29a	Puturosul	98.26	0.906	0.7826	0.0170	0.0423	0.000414	0.000037	0.012	< 0.000001	nd	2.29	10.11	2.33
29b	Puturosul Sud	95.63	1.975	2.3557	0.0052	0.0297	0.001374	0.000009	< 0.005	0.000009	−4.7	nd		
30	Bodoc Pella	99.21	0.576	0.0253	0.0102	0.1789	< 0.000005	0.000053	< 0.005	< 0.000001	−4.16	0.42	0.83	0.18
32	Balvanyus	97.97	0.896	1.0761	0.0170	0.0454	0.000624	0.000149	0.006	0.000004	nd	4.48	163.00	4.49
36	Slanic	99.35	0.291	0.2642	0.0027	0.0426	0.000029	0.000014	0.045	< 0.000001	−2.98	0.33	39.00	0.33
45a	Andreasu	1.22	0.186	98.5124	0.0023	0.0600	0.000479	0.000216	< 0.005	< 0.000001	nd	0.03	29.80	0.02
45b	Andreasu	1.02	2.311	96.1502	0.0077	0.1557	0.001313	0.000333	< 0.005	< 0.000001	nd	nd		
57	Perla Casinului	99.84	0.131	0.0020	0.0042	0.2701	0.002697	0.000342	< 0.005	< 0.000001	−2.56	1.52	0.79	1.80
61	Cavasna Mofette	32.85	55.119	0.0250	0.6310	7.4046	0.000442	< 0.000001	< 0.005	< 0.000001	nd	nd		
68	Ozunca Bai	98.62	0.915	0.0050	0.0159	0.3170	< 0.000005	< 0.000001	< 0.005	< 0.000001	−2.22	nd		
72	Berca	0.77	0.381	98.7662	0.0045	0.0169	0.000208	< 0.000001	< 0.005	< 0.000001	nd	0.06	32.94	0.05

$R_m = {}^3He/{}^4He$ measured.
$^{a3}He/{}^4He$ as R_m / R_a, corrected for air contamination using He/Ne ratio.

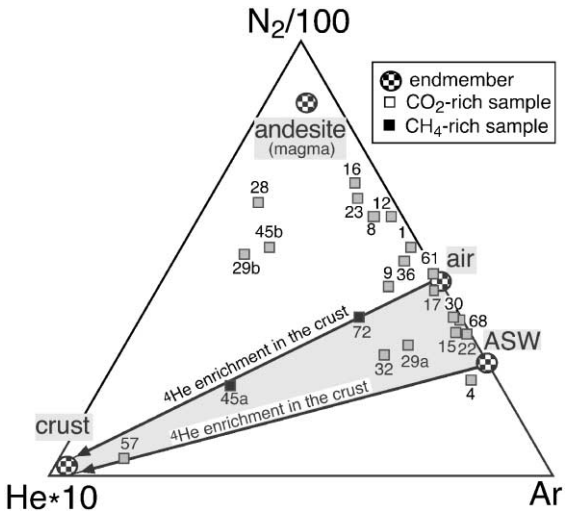

Fig. 5. Relative $N_2/100$–He×10–Ar compositions in the gas samples investigated (after Giggenbach et al., 1983).

The $^3He/^4He$ ratios measured in 17 selected gas samples are reported in Table 2 as R_m/R_a, where R_m is the measured $^3He/^4He$ ratio and R_a is the ratio in the atmosphere ($^3He/^4He = 1.39 \times 10^{-6}$; Mamyrin and Tolstikhin, 1984). Apart from the two CH_4-rich samples that have R_m/R_a values typical of crustal gases (0.02 and 0.06 in nos. 45a and 72, respectively), the gas samples from both the Harghita Mountains and Slanic areas record considerable quantity of mantle-derived ^3He. In particular, R_m/R_a varies from 0.28 at Slanic (no. 38) to 4.62 at Balvanyus (no. 32). If we consider a value of $R_m/R_a = 6.1–6.7$ for the European lithospheric mantle (Dunai and Baur, 1995), the high value found at Balvanyus (in an independent dacite dome close to the Ciomadul volcano where the most recent eruption in the whole Carpathian arc took place) and at minor extent in sample nos. 8, 15, 23, 28, and 29a, we may suggest

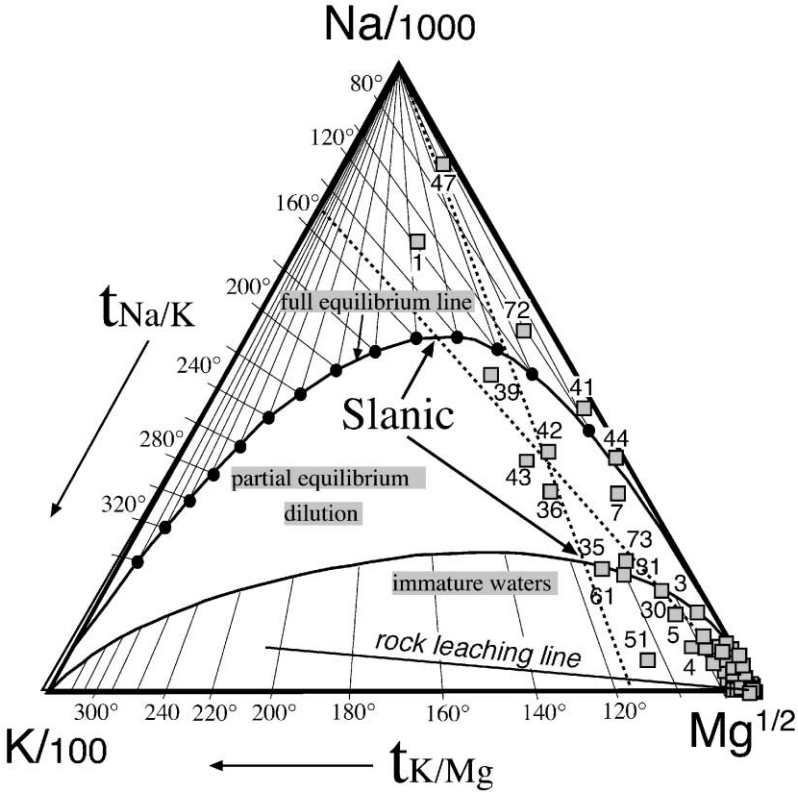

Fig. 6. Geothermometric evaluation of water samples using the Giggenbach (1988) approach. The hottest samples investigated are those emerging in the Slanic area (#35–44), where a deep 120- to 150-°C temperature can be evaluated.

the presence of high ^{3}He flux (> 50% of the total flux) from deep-seated active fault systems tracing the presence of still degassing magma-hosting chambers cooling down at depth.

6. Geothermometry

Although only two low-temperature thermal (> 20 °C) spring waters (nos. 12 and 67) are present in the western part of the study area, the diffuse emission of CO_2 at the surface would suggest the presence of active hydrothermal systems somewhere at depth within the volcanic chain. Dilution of hot rising hydrothermal fluids, if it occurs, may mostly be due to both the local high spring rainfall rate and spring and summer melting of the snow cap that accumulated during winter. Melted snow easily infiltrates during spring with the spring rainfalls but, because both rain and snow consist of very low-salinity waters, such a dilution, even if it causes a strong temperature drop of possible deep waters, should not affect significantly the relative proportion of cations in the rising deep-seated solutions.

With this limitation, we have applied the Giggenbach (1988) geothermometric approach by using the slow re-equilibrating Na/K geothermometer in the liquid phase and the fast re-equilibrating K^2/Mg geothermometer (Giggenbach et al., 1983). The graphical resolution of the combined geothermometers, together with the full equilibrium line of theoretical compositions at increasing temperature of solutions in equilibrium after secondary re-crystallization of minerals in a hydrothermal alteration system, the field of partial equilibrium or dilution, and the field of immature waters are reported in Fig. 6. The great majority of samples lie near the Mg corner and/or along the low-temperature area of the full

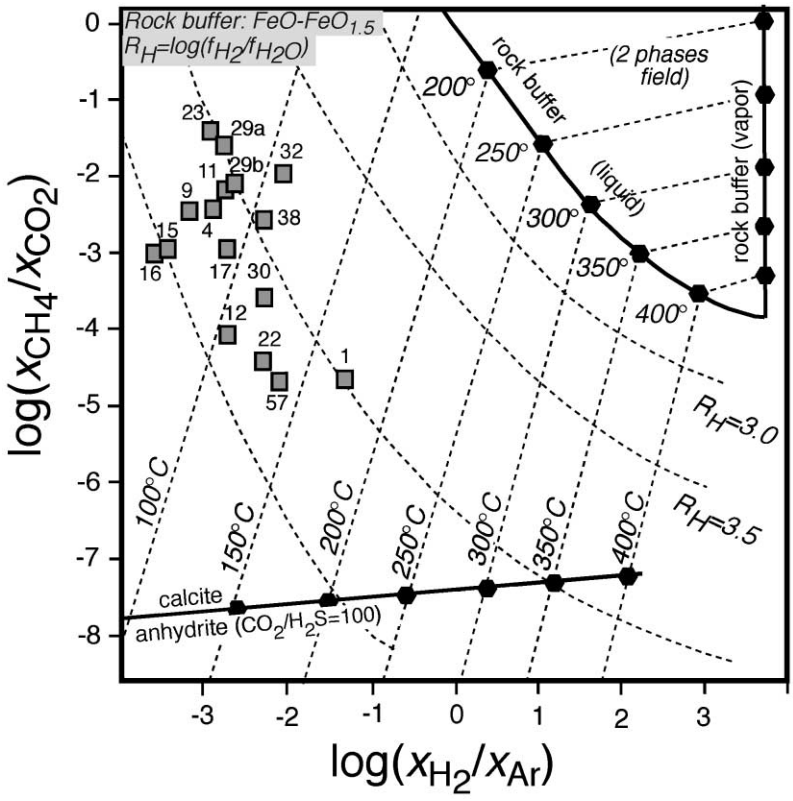

Fig. 7. Geothermometric evaluation of gas samples using CH_4, CO_2, H_2, and Ar relative concentration (after Giggenbach, 1993). See text.

equilibrium line, suggesting low K/Mg temperatures (< 100–120 °C) of any likely reasonably deep reservoirs at depth (< 2000–3000 m). Very saline water samples (nos. 1, 47, and 72) lie near the Na corner because the salinity is due to halite dissolution, whereas water–rock interaction processes can be considered negligible. Samples from Slanic (nos. 35–44), lying in the partial equilibrium–dilution sector in Fig. 6, can be regarded as the only waters with a likely deeper origin, the K/Mg equilibration temperatures being ca. 120–140 °C. As these springs clearly emerge along an important regional fault (along the Trotus river in Fig. 1), mixing processes with merging saline end members associated to the oil fields present nearby (SE of the springs) cannot be ruled out.

Temperatures lower than 150 °C are also derived when geothermometers through gas–gas reactions, such as the combined CH_4/CO_2 and H_2/Ar geothermometers, are considered (Fig. 7; Giggenbach, 1993). As in other areas of the world where hydrothermal systems are not present at shallow depth, the compositions of gas samples in the Eastern Carpathians are far from being representative of any deep fluid-equilibrated environment. In particular, hydrogen very fast re-equilibrates during the temperature drop along the rising path from any deep hydrothermal system to the surface; and Fig. 7 suggests that substantial oxidation of H_2 has occurred along the path from the source of the gas phase to the surface at relatively low temperature (< 100–150 °C) in systems likely characterised by one single-liquid phase.

The fact that possible deep temperatures suggested by liquid and gas geothermometers are similar (100–150 °C) indicates a common re-equilibrated source for deep components, or at least that the re-equilibration zone for both phases is attained in a system under similar thermodynamic constraints.

7. Discussion

7.1. Distribution patterns of some fluid chemical species at surface

The geothermometric analysis of components in both liquid and gas phases seems to suggest that the presence of any hydrothermal systems at shallow depth in the Eastern Carpathians can be excluded. This well agrees with the scarcity of thermal features (few low-temperature thermal springs and no fumaroles) at surface, even near the more recent Sfinta Ana (no. 28) crater of Ciomadul volcano. Despite this, the cross comparison of the isodistribution patterns among calculated water discharge pCO_2 (Fig. 8a), the $^3He/^4He$ ratio (R_m/R_a) in the gas phase (Fig. 8b), and heat flow (in mW m^{-2}; Fig. 8c, redrawn after Veliciu, 1987) maps suggests that there is a clear uprising of deep fluids in the southernmost part of the CGH volcanic chain. Owing to the positive correlation between the above mentioned chemical and thermal parameters, as already observed in different tectonic regimes by Polyak and Tolstikhin (1985), it seems reasonable to hypothesise the presence of mantle magmas residing in the crust which have not yet completely cooled down.

By moving from this area towards the eastern flysch nappes in the main thrust belt and the foredeep areas, both CO_2 and ^3He decrease to values commonly found in areas of crustal thickening and/or in areas where compression prevails over extension (Minissale et al., 2000b). In particular, the CO_2-rich gas rising along the transcrustal fault system at Slanic (Sandulescu, 1984; Garbacea, 1997), not being associated to anomalous $^3He/^4He$ ratios (although its $R_m/R_a > 0.2$ suggests slight input of mantle gas; Marty et al., 1992), points to the presence of CO_2 production at depth not necessary related to the presence of rising mantle magmas.

7.2. Origin of CO_2

The origin of CO_2 in the Eastern Carpathians can be deduced from the $\delta^{13}C$ in CO_2 values (Table 2). Setting aside sample nos. 1 and 12 where the light $\delta^{13}C$ in CO_2 is likely caused by the production of CO_2 from the alteration of organic matter embedded in the sediments of the Transylvanian Neogene sedimentary sequence, the remaining samples show quite similar $\delta^{13}C$ values ranging from $-2.1‰$ to $-4.7‰$. Craciun et al. (1989, their Fig. 9 within) measured $\delta^{13}C$ values in the range $-6.0‰$ to $+2.0‰$ in free CO_2 of mineral water samples in the Eastern Carpathian volcanic zone. Such values overlie the fields of mantle-derived CO_2 (-4.0 to -7.0; Rollinson,

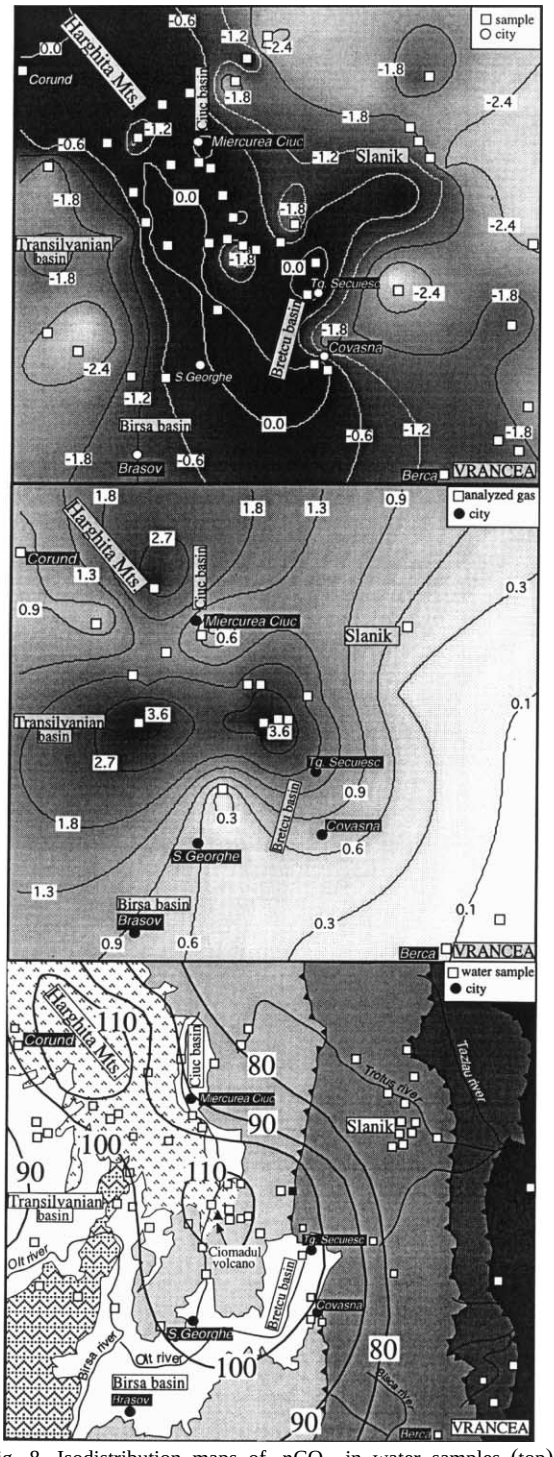

Fig. 8. Isodistribution maps of pCO_2 in water samples (top), $^3He/^4He$ ratio (as R_m/R_a) in the gas phase (middle), and heat flow (in mW m^{-2}) (redrawn after Veliciu, 1987) (see text).

1993) and CO_2 derived from alteration and hydrothermal metamorphism of marine carbonates (-2.0 to $+2.0$; Rollinson, 1993), suggesting for the Eastern Carpathians that CO_2 derived from these two main sources likely mixed at deep levels in the crust.

These two sources are not likely evenly distributed within the crust. Hydrothermal metamorphism of limestones at depth might in fact be related to the presence of a Miocene–Pliocene subducted slab "baked" by andesitic magmas. However, subducted limestones, if sufficiently deep, could locally generate CO_2 without contacting any ^{3}He-rich mantle component but simply because of the thermal gradient that in active margins is always high (Fig. 8c). In addition, hydrolysis of limestones is likely to occur even at relatively low temperature (< 150 °C; Kissin and Pakhomov, 1967).

Although measurements of flow rate of springs and associated CO_2 could not be carried out during the field sessions, the number of springs and wells characterised by the presence of CO_2-rich emissions (soda springs) is in some areas very high (Dragos, 1965a,b). The quantity of such non magmatic CO_2 that contributes to the carbon cycle is likely to be very important for the world CO_2 balance calculation, and may account together with similar areas, such as the Northern Apennines, for the world budget deficit reported by Berner et al. (1983).

As far as the $^3He/^4He$ (R_m/R_a) ratios in the gas samples are concerned, they seem to validate the conclusions based on the carbon isotopes in CO_2. As already stated, assuming a R_m/R_a ratio of 6.1–6.7 for the European lithospheric mantle (Dunai and Baur, 1995), the values found in Harghita Mountains gas samples suggest that more than 50% of total He can be related to mantle degassing. Such mantle gas can either: (i) directly rise from the mantle or (ii) originate from a mantle-derived magma reservoir residing and still degassing in the crust. The magma chamber of the youngest Ciomadul volcano could be a possible source. Such a hypothesis has already been proposed based on local seismicity and attenuation of teleseismic waves (Lazarescu, written communication, 1984; Szakacs and Seghedi, 1993).

Generation of CO_2 inside the crust, with or without the presence of contacting mantle magmas and their associated thermal anomalies, could justify the fact that the R_m/R_a values in the gas samples from

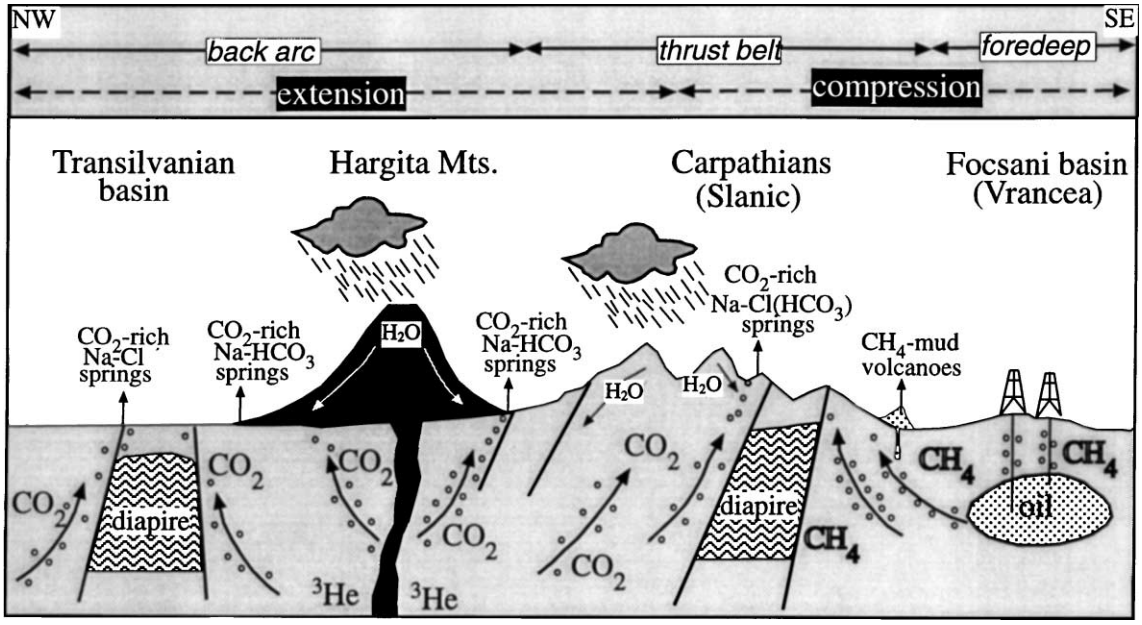

Fig. 9. Conceptual fluid geochemical cross-section across the southeast Carpathians (see text).

Eastern Carpathians are more variable with respect to the $\delta^{13}C$ values in CO_2. Generally speaking, the higher the R_m/R_a values, the closer the degassing magma. On the other hand, dilution by crustal radiogenic ^4He can be envisaged when moving outside the magmatic areas.

7.3. Relation between fluids and active tectonics

Geochemical investigations of natural fluids emerging across the Northern Apennines (Minissale et al., 2000b), in an area with similar tectonic setting and fluid distribution as the Eastern Carpathians, have shown that the Transilvanian Basin can be compared to the peri-Tyrrhenian area (Polyak et al., 1979; Minissale et al., 1999), with comparably high heat flow, and gas emissions with high CO_2 concentration and relatively high $^3He/^4He$ ratios. At the same time, the Foscani basin in Romania and the foredeep area of the Northern Apennines (Po Valley and Adriatic coast) are characterised by gases with CH_4-rich mud volcanoes and crustal $^3He/^4He$ ratios. These observations can also be extended to other Alpine–Himalayan folding belts, as reported by Polyak et al. (2000) by studying $^3He/^4He$ ratios in subsurface fluids from the Northern Caucasus.

A conceptual model of the Eastern Carpathians fluid circulation is illustrated in Fig. 9 where an idealised NW–SE cross-section from the Transylvanian Basin to the Vrancea seismic region is shown. Diapire intrusions of synorogenic halite deposits (Mrazec, 1907) characterise both sectors. CO_2 seems to be related to the presence of both andesite volcanoes and/or extensional tectonics in the Harghita Mountains area. Such deep-originated CO_2 in its motion to the atmosphere spreads at shallow depth in cold aquifers that turn their composition to be Na–HCO_3.

Carbon dioxide emission is enhanced along active plate margins, as was early recognised by Barnes et al. (1978), and its degassing contribution from the mantle was suggested by several authors (e.g. Javoy et al., 1982; Barnes et al., 1988). Nevertheless, several studies have suggested the contribution of subducted material to the production of CO_2 during metamorphism in orogenic areas (e.g. Kerrick and Caldeira, 1997). The present study emphasises the fact that the inner extensional sector of an active plate boundary affected by recent subduction, such as the Eastern Carpathians, is a CO_2-producing (mainly of nonmagmatic origin) area, as observed in other Alpine–Himalyan belts such as those, for ex-

ample, in the Northern Apennines and Northern Caucasus. Furthermore, the CO_2-rich gases are normally characterised by higher $^3He/^4He$ ratios when compared to CH_4- and N_2-rich gases that show low and highly variable $^3He/^4He$ ratios, respectively (e.g. Minissale et al., 1997; Polyak et al., 2000).

In the Eastern Carpathians, the area characterised by CO_2-rich springs and mofettes is relatively large (Fig. 1), including hundreds of springs; therefore, the contribution of CO_2 to the atmosphere cannot be considered negligible. Free CO_2 in mineral waters amounts up to over 2 g/l in average for individual springs in south Harghita area (Airinei et al., 1989).

The previously discussed genetic relationship among the relative high R_m/R_a ratios, the heat-flow values, the andesitic volcanism, and the $\delta^{13}C$ in CO_2 values of about $-4.0‰$, suggests that CO_2 might partly have a mantle origin as proposed by Barnes et al. (1988). Nevertheless, if we consider that subducted limestones and organic-rich sediments can reach depth where their thermal decomposition would produce both isotopically light CO_2 from organic matter and heavy CO_2 from limestones, their mixing could generate CO_2 with similar $\delta^{13}C$ values of those measured in the Harghita Mountains. This would also explain the mean $\delta^{13}C$ value measured in the Harghita Mountains and would not imply the rising of CO_2 from the mantle but only recycling of subducted sediments triggered by the thermal anomaly generated by the intrusion and permanence at depth of andesitic magmas.

Along the thrust belt area, a deep fault (Trotus Fault along the Trotus river in Fig. 1) near the Slanic town carries to the surface relatively deep saline fluids with relative small mantle ^3He signature ($R_m/R_a = 0.28$ in no. 36). As it is not far from the Harghita Mountains area, such ^3He could derive from lateral escape of the easternmost volcanic conduits.

In the eastern stable foredeep area (Focsani basin), characterised by the presence of oil fields and mud volcanoes, rising of deep CO_2 and ^3He has not been discovered even in the seismic Vrancea region. Although the presence of active subduction in Vrancea is not well assessed (Bleahu, 1985; Garbacea, 1997; Seghedi et al., 1998), absence of any rising deep-seated fluid suggests that the area is still under compression, since the deep earthquakes generated in the astenosphere (e.g. Oncescu et al., 1984) are not related to any extensional structure in the overlying lithosphere.

8. Concluding remarks

The mineral, mostly cold, water and gas discharges in the Eastern Carpathians spread from the Transylvanian Basin to the west through the southernmost CGH volcanic chain, flysch nappes, and the foredeep area (Focsani depression) to the east.

The chemical features of the water springs investigated point to a relatively strong influence by the Miocene saline diapires, which locate from the west to the east, partly masking the original (though meteoric-originated) deep composition. On the other hand, the gas composition strongly differs from the west (CO_2 rich) to the east (CH_4 rich). This sharp variation corresponds to the different tectonic regimes affecting the Transylvanian Basin and the Harghita Mountains volcanic area (CO_2 domain with high $^3He/^4He$ ratios) and the flysch and Focsani depression (CH_4 domain with low $^3He/^4He$ ratios), that is extensional and compressive areas, respectively. This would seem to suggest that the fluid composition is likely strictly controlled by the geodynamic and structural regime as observed in a similar geological context such as that of the Northern Apennines (Italy), although further studies need to validate such a hypothesis.

Acknowledgements

This research was partly supported by the Ministries of Foreign Affairs of Italy and Romania as part of the scientific collaboration between the two countries. We are grateful to D. Badescu, S. Grigorescu, and S. Veliciu (Geological Institute of Romania, Bucharest) for their help during the two field campaigns. C. Baciu (Department of Geology, Cluj-Napoca, Romania) is thanked for providing useful references to this work. Some gas samples have been analysed for main and isotopic composition by W.C. Evans (USGS, Menlo Park, CA, USA) to whom the authors express their gratitude.

The authors warmly thank I. Tolstichin, G. Chiodini, and E. Oelkers for their useful comments and suggestions to an early draft of the paper.

OV, AM, IS, and DI thank the PANCARDI igneous petrology group for the useful discussion during the PANCARDI workshops in the last 3 years.

References

Airinei, S., Pricajan, A., Faco, M., 1989. Contributii la cunoasterea ritmicitatii dioxidului de carbon liber din apele carbogazoase din partea interna a curburii Carpatilor Orientali. Stud. Teh. Econ., Ser. E 15, 5–16 (in Romanian).

Ball, J.W., Nordstrom, D.K., 1991. User's manual for WATEQ4F with revised thermodynamic data base and test cases for calculating speciation of major, trace and redox elements in natural waters. U. S. Geol. Surv., Open-File Rep. 91-183, 189 pp.

Baltes, N., 1983. Hydrocarbon source rocks in Romania. Anu. Inst. Geol. Geofiz. (Bucharest, Romania) LX, 265–270.

Barnes, I., Irwin, W.P., White, L.D., 1978. Global distribution of CO_2 and major zone of seismicity. U. S. Geol. Surv., Open-File Rep. 78-39, 12 pp.

Barnes, I., Evans, W.C., White, L.D., 1988. The role of mantle CO_2 in volcanism. Appl. Geochem. 3, 281–285.

Berner, R.A., Lasaga, A.C., 1989. Modeling the geochemical carbon cycle. Sci. Am. 260, 74–81.

Berner, R.A., Lasaga, A.C., Garrels, R.M., 1983. The carbonate–silicate geochemical cycle and its effect on atmospheric carbon dioxide over the past 100 million years. Am. J. Sci. 283, 641–683.

Bleahu, M., 1985. The magmatic arc of East Carpathians: discussion and proposal for interpretation. Rocz. Pol. Tow. Geol. 53, 23–31.

Brantley, S.L., Koepenick, K.W., 1995. Measured carbon dioxide emissions from Oldoinyo Lengai and the skewed distribution of passive volcanic fluxes. Geology 23, 933–936.

Chiodini, G., Frondini, F., Kerrick, D., Rogie, J., Parello, F., Peruzzi, L., Zanzari, R., 1999. Quantification of deep CO_2 fluxes from central Italy. Examples of carbon balance for regional aquifers and of soil diffuse degassing. Chem. Geol. 159, 205–222.

Chiodini, G., Frondini, F., Cardellini, C., Parello, F., Peruzzi, L., 2000. Rate of diffuse carbon dioxide Earth degassing estimated from carbon balance of regional aquifers: the case of central Apennine, Italy. J. Geophys. Res. 105, 8423–8434.

Craciun, P., Bandrabur, T., 1993. Some hydrogeochemical features of the geothermal areas related to the Neogene volcanics in the Harghita Mountains (Romania). Bull. A.H.R. (Bucharest, Romania) II (1), 11–19.

Craciun, P., Barnes, I., Bandrabur, T., 1989. Stable isotopes in hydrogeothermal structures in Romania. Stud. Teh. Econ., Ser. E 15, 17–39.

Craig, H., 1961. Isotopic variations in meteoric waters. Science 133, 1702–1703.

Csontos, L., 1995. Tertiary tectonic evolution of the intra-Carpathian area: a review. Acta Volcanol. 7, 1–13.

Dragos, V., 1965a. Privire generala asupra geologiei si a apelor mineralizate din regiunea Cluj. Apele minerale si namolurile terapeutice din R.P.R. Editura Med. II, 162–178.

Dragos, V., 1965b. Privire generala asupra geologiei si a apelor mineralizate din regiunea Maramures. Apele mineralizate si namolurile terapeutice din R.P.R. Editura Med. II, 275–286.

Drever, J.L., 1982. The Geochemistry of Natural Waters. Prentice-Hall, Englewood Cliffs, NJ, USA, pp. 82–85.

Duchi, V., Minissale, A., Rossi, R., 1986. Chemistry of thermal springs in the Larderello geothermal field. Appl. Geochem. 1, 659–667.

Dunai, T.J., Baur, H., 1995. Helium, neon and argon systematics of the European subcontinental mantle: implications for its geochemical evolution. Geochim. Cosmochim. Acta 59, 2767–2783.

Garbacea, R., 1997. The Pliocene to recent tectonic evolution of the Eastern Carphatians. Tub. Geowiss. Arb. 35, 136 pp.

Gatt, J.R., Carmi, I., 1970. Evolution of the isotopic composition of atmospheric waters in the Mediterranean Sea area. J. Geophys. Res. 75, 3032–3048.

Gerlach, T.M., 1991. Present day CO_2 emissions from volcanoes. Eos Trans. 72, 249–255.

Giggenbach, W.F., 1975. A simple method for the collection of volcanic gas samples. Bull. Volcanol. 39, 132–145.

Giggenbach, W.F., 1988. Geothermal solute equilibria: derivation of Na–K–Ca–Mg geoindicators. Geochim. Cosmochim. Acta 52, 2749–2765.

Giggenbach, W.F., 1993. Redox control of gas compositions in Philippine volcanic–hydrothermal systems. Geothermics 22, 575–587.

Giggenbach, W.F., Gonfiantini, R., Jangi, B.L., Truesdell, A.H., 1983. Isotopic and chemical composition of Parbati Valley geothermal discharges, NW-Himalaya. Geothermics 12, 199–222.

Gonfiantini, R., 1986. Environmental isotopes in lake studies. In: Fritz, P., Fontes, J.Ch. (Eds.), Handbook of Environmental Isotope Geochemistry. Elsevier, Amsterdam, pp. 113–168.

Javoy, M., Pineau, F., Allègre, C.J., 1982. Carbon geodynamic cycle. Nature 300, 171–173.

Juvigne, E., Gewelt, M., Gilot, M., Hurtgen, C., Seghedi, I., Szakàcs, A., Hadnagy, A., Gabris, G., Horvàth, F., 1994. Une eruption vieille d'environ 10,700 ans (14C) dans le Carpathes Orientales (Roumanie). C. R. Acad. Sci. (Paris, France) 318, 1233–1238.

Kerrick, D.M., Caldeira, K., 1997. Metamorphic CO_2 degassing from orogenic belts. Chem. Geol. 145, 213–232.

Kerrick, D.M., McKibben, M.A., Seward, T.M., Caldeira, K., 1995. Convective hydrothermal CO_2 emission from high heat flow regions. Chem. Geol. 121, 285–293.

Kissin, I.G., Pakhomov, S.I., 1967. The possibility of carbon dioxide generation at depth at moderately low temperature. Dokl. Akad. Nauk SSSR 174, 451–454.

Magro, G., Pennisi, M., 1991. Noble gases and nitrogen: mixing and temporal evolution in the fumarolic fluids of Vulcano, Italy. J. Volcanol. Geotherm. Res. 47, 237–247.

Mamyrin, B.A., Tolstikhin, I.N., 1984. Helium isotopes in nature. In: Fyfe, W.S. (Ed.), Developments in Geochemistry, Series 3. Elsevier, Amsterdam.

Marty, B., Tolstikhin, I.N., 1998. CO_2 fluxes from mid-ocean ridges, arc and plumes. Chem. Geol. 145, 233–248.

Marty, B., O'Nions, R.K., Oxburgh, E.R., Martel, D., Lombarsi, S., 1992. Helium isotopes in Alpine regions. Tectonophysics 206, 71–78.

Mason, P.R.D., Downs, H., Thirlwall, M.F., Seghedi, I., Szakàcs, A., Lowry, D., Mattey, D., 1996. Crustal assimilation as a major petrogenic process in the East Carphatians Neogene and Quaternary continental margin arc. J. Petrol. 37, 927–959.

Mason, P.R.D., Seghedi, I., Szakàcs, A., Downes, H., 1998. Magmatic constraints on geodynamic models of subduction in the East Carpathians. Tectonophysics 297, 157–176.

Mazor, E., 1991. Applied Chemical and Isotopic Groundwater Hydrology. New York Halstead Press, New York, 274 pp.

Minissale, A., Evans, W.C., Magro, G., Vaselli, O., 1997. Multiple source components in gas manifestations from north–central Italy. Chem. Geol. 142, 175–192.

Minissale, A., Vaselli, O., Tassi, F., Seghedi, I., Magro, G., Ioane, M., 1999. Fluid sources in orogenic areas, two examples: Northern Apennines and Eastern Carpathians. Proc. Europrobe (Pancardi) Meeting 99, 1–6 ott. Tulcea, Romania (abs.). Geoecomar, Bucharest.

Minissale, A., Vaselli, O., Chandrasekharam, D., Magro, G., Tassi, F., Casiglia, A., 2000a. Origin, evolution of "intracratonic" thermal fluids from central–western peninsular India. Earth Planet. Sci. Lett. 181, 377–394.

Minissale, A., Magro, G., Martinelli, G., Vaselli, O., Tassi, F., 2000b. A fluid geochemical transect in the Northern Apennines (central–northern Italy): fluid genesis and migration and tectonic implications. Tectonophysics 319, 199–200.

Moriya, I., Okuno, M., Nakamura, T., Ono, K., Szakàcs, A., Seghedi, I., 1996. Radiocarbon ages of charcoal fragments from the pumice flow deposits of the last eruption of Ciomadul volcano, Romania. Summaries of Research Using AMS at Nagoya University, vol. VII. Nagoya University Press, Nagoya, p. 255.

Mrazec, L., 1907. Despre cute cu simbure de strapungere. Bul. Soc. Stiinte (Bucuresti) 16 (in Romanian).

Oncescu, M.C., Burlacu, V., Anghel, M.M., Smalberger, V., 1984. Three-dimensional P-wave velocity image under the Carpathian Arc. Tectonophysics 106, 305–319.

Peltz, S., Vajdea, E., Balogh, K., Pecskay, Z., 1987. Contributions to the chronological study of the volcanic processes in the Calimani and Hargita Mountains (East Carpathians, Romania). Dari Seama Sedintelor-Inst. Geol. Geofiz. 72–73 (1), 323–338.

Pesckay, Z., Edelstien, O., Seghedi, I., Szakacs, A., Kovacs, M., Crihan, M., Bernard, A., 1995. K–Ar datings of Neogene–Quaternary calc-alkaline volcanic rocks in Romania. Acta Volcanol. 7, 53–61.

Polyak, B.G., Tolstikhin, I.N., 1985. Isotopic composition of the Earth's helium and the problem of the motive forces of tectonogenesis. Chem. Geol. 52, 9–33.

Polyak, B.G., Tolstikhin, I.N., Yakutseni, V.P., 1979. Isotopic composition of helium and terrestrial heat flow: geochemical and geophysical aspects of tectonogensis. Geotektonica 5, 3–23 (in Russian).

Polyak, B.G., Tolstikhin, I.N., Kamensky, I.L., Yakolev, L.E., Marty, B., Cheshko, A.L., 2000. Helium isotopes, tectonics and heat flow in the Northern Caucasus. Geochim. Cosmochim. Acta 64, 1925–1944.

Radulescu, D., Tatrascu, S., Bellon, H., 1972. Pliocene geomagnetic epochs. New evidence of reversed polarity around the age of 7 m.y. Earth Planet. Sci. Lett. 14, 114–128.

Radulescu, D., Peter, E., Stanciu, C., Stefanescu, M., Veliciu, S., 1981. Asupra anomaliilor geotermice din sudul Muntilor Harghita. Stud. Cercet. Geogr. Geofiz., Ser. Geol. 26 (2), 169–184.

Radulescu, D., Sandulescu, M., Veliciu, S., 1983. A geodynamic model of the East Carpathians and the thermal field in the lithosphere. Anu. Inst. Geol. Geofiz. LXIII, 135–144.

Rogie, J.D., Kerrick, D.M., Chiodini, G., Frondini, F., 2000. Flux measurements of nonvolcanic CO_2 emission from some events in central Italy. J. Geophys. Res. 105, 8435–8445.

Rollinson, H., 1993. Using Geochemical Data. Longman, London, UK, 352 pp.

Roman, C., 1970. Seismicity in Romania, evidence for the sinking lithosphere. Nature 233, 1176–1178.

Royden, L.H., 1993. The tectonic expression slab pull at continental convergence boundaries. Tectonics 12, 303–325.

Sandulescu, M., 1984. Geotectonica Romaniei. Editura Tehnica, Bucuresti, Romania, 336 pp.

Seghedi, I., Balintoni, I., Szakàcs, A., 1998. Interplay of tectonics and Neogene post-collisional magmatism in the intracarpathian area. Lithos 45, 483–499.

Seward, T.M., Kerrick, D.M., 1996. Hydrothermal CO_2 emission from Taupo volcanic zone, New Zealand. Earth Planet. Sci. Lett. 139, 105–113.

Szakacs, A., Seghedi, I., 1993. The youngest volcanism in Eastern Europe. Is it still active? Abstract. Part I. Ann. Geophys. (Berlin, Germany) 11 (Suppl. I), C81.

Veliciu, S., 1987. Geothermics of the Carpathian area. Anu. Inst. Geol. Geofiz. 67, 81–116.

Veliciu, S., 1988. Contributii privind prospectiunea geotermica a apelor termale cu aplicatie in R.S. Romania. Stud. Teh. Econ., Ser. D (Inst. Geol. Geofiz.) 15, 85–201 (in Romanian).

Williams, S.N., Schaefer, M.L., Calvache, V., Lopez, D., 1992. Global carbon dioxide emission to the atmosphere by volcanoes. Geochim. Cosmochim. Acta 56, 1770–1992.

Xu, S., Nakai, S., Wakita, H., Wang, X., Feng, X., 1997. Effects of hydrothermal processes in the chemical and isotopic composition of mantle-derived gases in SE China. Geothermics 26, 179–192.

Zweigel, P., 1997. The Tertiary tectonic evolution of the Eastern Carpathians (Romania): orogenic arc formation in response to microplate movements. Tub. Geowiss. Arb., Reihe A 33, 156 pp.